The Zeeman splitting of quasi-one dimensional electron subbands

1992 J. Phys.: Condens. Matter 4 4499

(http://iopscience.iop.org/0953-8984/4/18/016)

J. Phys.: Condens. Matter 4 (1992) 4499–4508. Printed in the UK

The Zeeman splitting of quasi-one-dimensional electron subbands

N C Constantinou, M Masale and D R Tilley
Department of Physics, University of Essex, Colchester CO4 3SQ, UK

Received 13 December 1991, in final form 6 February 1992

Abstract. The subband energy levels of an electron confined in one dimension by a cylindrically symmetric square well potential (both infinite and finite) are investigated within the effective-mass approximation as a function of magnetic field applied along the cylinder axis. For small fields the doubly degenerate states ($|m| > 0$), where m is the azimuthal quantum number, are Zeeman split with subbands having $m > 0$ shifting to higher energies whilst those with $m < 0$ initially decrease in energy. A minimum in the energy of the negative-m states is predicted. This minimum occurs whatever the specific form of the confining potential, the only proviso being that it is cylindrically symmetric. This effect is intimately related to the number of elementary flux quanta $\Phi_0(= h/e)$ contained within the electron's cyclotron orbit.

1. Introduction

The dynamics of electrons in a uniform magnetic field has been of interest since the earliest days of quantum mechanics. The motion of a free electron is discussed in standard texts, e.g. [1], while Harper [2] discusses Bloch electrons. With the development of interest in low-dimensional structures, attention turned to the dynamics of electrons in quantum wells. With the field perpendicular to the walls, the motion is the usual quantized cyclotron orbit in the plane of the well. However, when the field is parallel to the walls, the boundary conditions at the walls play a crucial part, and in addition the eigenvalues become a function of wavevector component in the plane and transverse to the magnetic field. Klama [3] gives the formulation of the problem for infinite walls and shows that the eigenfunctions can be written in terms of Weber functions. Lee *et al* [4] extend this treatment to the case where the walls are finite, although they use the boundary conditions that ψ and $\boldsymbol{n} \cdot \nabla\psi$ are continuous rather than the effective-mass boundary conditions that apply in simple cases for semiconductor quantum well systems [5]. A number of authors, the most recent being Mitrović *et al* [6], develop self-consistent treatments for systems in which a finite density of electrons modifies the single-electron potential.

Since the prediction by Sakaki [7] of the enhancement of the low-temperature mobility when carriers are confined in two spatial dimensions, there has been a great deal of interest in the physics of quasi-one-dimensional semiconductor systems [8–10]. Until very recently, in contrast to the case of the analogous two-dimensional system, wire dimensions have been such that it was difficult to observe occupation of only the lowest subband level (the so-called extreme quantum limit) with many subbands being

0953-8984/92/184499+10$04.50

normally occupied. The work of Plaut *et al* [11] was the first to demonstrate the one-dimensional quantum limit at zero magnetic field, and they presented results for the subband energy variation as a function of perpendicular magnetic field. The electric confining potential often assumed is parabolic, although self-consistent calculations by Laux *et al* [12] demonstrate a confining potential that has a form intermediate between that of a parabolic and a square well. In fact, the square-well potential with finite walls is useful in interpreting some of the measured subband levels [11]. A recent paper by Makar *et al* [13] deals with a related problem. In their work they consider the density of electronic states for a metallic cylindrical shell when subjected to an axial static magnetic field. This is an interesting problem to which we return in section 5.

In view of the above considerations, it is timely to consider the one-dimensional analogue of the work by Klama [3]. Specifically, we consider a cylindrical quantum wire (GaAs) embedded in a host material ($Al_xGa_{1-x}As$) with the magnetic field applied along the cylinder axis. This type of structure was proposed by Iafrate *et al* [14] and is similar to structures fabricated by Gibert *et al* [15]. The subband energy levels in the absence of a magnetic field have been obtained recently by Constantinou and Ridley [16].

In this paper we derive the single-electron energy spectrum for a cylinder in a uniform applied field B parallel to the axis. For ease of presentation we deal first with the case of an infinite potential step at the outer radius of the wire, then turn to a finite step across which effective-mass boundary conditions are applied. Although the former is a limiting case of the latter, it is helpful to survey the results separately. The key parameter is the ratio a_c/R, where a_c is the cyclotron radius for angular momentum $\hbar$:

$$a_c^2 = \hbar/eB \tag{1}$$

and R is the cylinder radius. In the absence of any other potential, the magnetic field may be seen as confining the electron to the classical orbit of radius a_c. Thus if $a_c/R \ll 1$, the electron is strongly confined by the magnetic field, confinement in the cylinder is irrelevant, and the spectrum is the quantized cyclotron energy

$$E_n = \left(n + \tfrac{1}{2}\right)\hbar\omega_c \qquad n = 0, 1, 2, 3, \ldots \tag{2}$$

where

$$\omega_c = eB/\mu \tag{3}$$

is the cyclotron frequency and μ the electron's effective mass. Conversely, for a weak field, $a_c/R \gg 1$, the magnetic field confinement is unimportant and the energy spectrum of an electron in a cylinder is recovered.

In section 2 we review the Schrödinger equation and energy spectrum for the infinite step in the absence of a field, since this does not come out in a very transparent way as the limit of the spectrum with the field included. The corresponding calculation for a finite step is given by [16] and will not be repeated here. Section 3 contains the first main calculation, for the cylinder with an infinite potential step in the presence of a magnetic field, while section 4 deals with the finite step. Some conclusions are presented in section 5.

2. Zero magnetic field

In cylindrical polar coordinates (ρ, z, ϕ) the eigenfunction is

$$\psi = A\chi(\rho)\exp(\mathrm{i}kz)\exp(\mathrm{i}m\phi) \qquad m = 0, \pm 1, \pm 2, \ldots \tag{4}$$

where A is a normalization factor and the radial function $\chi(\rho)$ satisfies

$$\rho^2 \frac{\mathrm{d}^2\chi}{\mathrm{d}\rho^2} + \rho\frac{\mathrm{d}\chi}{\mathrm{d}\rho} + \left[(2\mu E/\hbar^2)\rho^2 - m^2\right]\chi = 0 \tag{5}$$

with the total energy E_{T} given by

$$E_{\mathrm{T}} = \hbar^2 k^2/2\mu + E. \tag{6}$$

Here k is the axial wavevector and E the subband energy. Equation (5) is Bessel's equation, the solution that is bounded at $\rho = 0$ being

$$\chi = J_m(q\rho) \tag{7}$$

where

$$q^2 = 2\mu E/\hbar^2. \tag{8}$$

For an infinite wall at radius R, the boundary condition is $\chi(R) = 0$, so the eigenvalue equation is

$$J_m(qR) = 0. \tag{9}$$

Equations (8) and (9) together show that the radial eigenvalue spectrum is

$$E_{mp} = z_{mp}^2\hbar^2/2\mu R^2 \tag{10}$$

where z_{mp} is the pth root of the mth Bessel function $J_m(z)$. As might be expected from simple uncertainty principle arguments, E scales like $1/R^2$ for all m and p. Note that the eigenstates are doubly degenerate for $m \neq 0$. As mentioned, the extension of this calculation for a finite wall is given by [16].

3. Applied magnetic field, infinite step

For a uniform field $\boldsymbol{B}$ in the z direction, the vector potential may be taken as

$$A_\rho = A_z = 0 \qquad A_\phi = \tfrac{1}{2}B\rho \tag{11}$$

so the Hamiltonian is (with $\hat{p} = -\mathrm{i}\hbar\nabla$ and Q the charge) given by

$$\hat{H} = (\hat{p}_\rho^2 + \hat{p}_z^2)/2\mu + \left(\hat{p}_\phi - \tfrac{1}{2}QB\rho\right)^2/2\mu. \tag{12}$$

The eigenfunction may still be written in the form (4), but the radial function now satisfies

$$\frac{\mathrm{d}}{\mathrm{d}\rho}\left(\rho\frac{\mathrm{d}\chi}{\mathrm{d}\rho}\right)+\rho\left[\frac{2\mu}{\hbar^2}E-\left(\frac{QB}{2\hbar}\right)^2\rho^2-\left(\frac{m}{\rho}\right)^2+\frac{mQB}{\hbar}\right]\chi=0 \quad (13)$$

where the subband energy E is again related to the total energy by equation (6). We are interested in the electron states, and as such set the charge Q to $-e$. It is clear from equation (13) that a change of sign in the charge is equivalent to a change of sign in the azimuthal quantum number m. Equation (13) may be written as

$$\xi^2\frac{\mathrm{d}^2\chi}{\mathrm{d}\xi^2}+\xi\frac{\mathrm{d}\chi}{\mathrm{d}\xi}+\left[E\xi/\hbar\omega_c-\tfrac{1}{4}(\xi+m)^2\right]\chi=0 \quad (14)$$

where the dimensionless variable ξ has been defined by

$$\xi=\rho^2/2a_c^2 \quad (15)$$

and the eigenvalue is given by (6). The substitution [1]

$$\chi=A\,\exp(-\xi/2)\xi^{|m|/2}W(\xi) \quad (16)$$

leads to

$$\xi\frac{\mathrm{d}^2W}{\mathrm{d}\xi^2}+(b-\xi)\frac{\mathrm{d}W}{\mathrm{d}\xi}-aW=0 \quad (17)$$

which is the canonical form of Kummer's equation for the confluent hypergeometric function [17].

The solution of (17) that is bounded at $\rho=0$ is

$$W(\xi)=M(a,b,\xi) \quad (18)$$

where

$$a=\tfrac{1}{2}-E/\hbar\omega_c+\tfrac{1}{2}|m|+\tfrac{1}{2}m \quad (19)$$

and

$$b=|m|+1 \quad (20)$$

are the parameters of the Kummer function in standard notation. The boundary condition $\Psi=0$ for $\rho=R$ therefore leads to the eigenvalue equation

$$M(a,b,R^2/2a_c^2)=0. \quad (21)$$

For given R/a_c and given azimuthal quantum number m (i.e. given b), this determines the eigenvalue E since it determines a. It is seen from (19) that the sign of m enters the eigenvalue, as can be expected on simple physical grounds. For an infinite medium, $R\to\infty$, equation (21) is replaced by the requirement that M be bounded as $R^2/2a_c^2 \to \infty$. As discussed by Landau and Lifshitz, this simply means that a is a negative integer,

$$a = -l \qquad l = 0, 1, 2, \ldots \tag{22}$$

leading to the standard result

$$E = \left(n + \tfrac{1}{2}\right)\hbar\omega_c \tag{23}$$

with

$$n = l + m \qquad \text{for } m > 0 \tag{24}$$

$$n = l \qquad \text{for } m \leqslant 0. \tag{25}$$

For $a_c/R \gg 1$, on the other hand, confinement by the magnetic field is unimportant, and the eigenvalue spectrum of (10) is recovered.

Numerical evaluation of the formulae of this section requires subroutines for the confluent hypergeometric functions. These are not available in standard libraries so we have employed their integral representations [17].

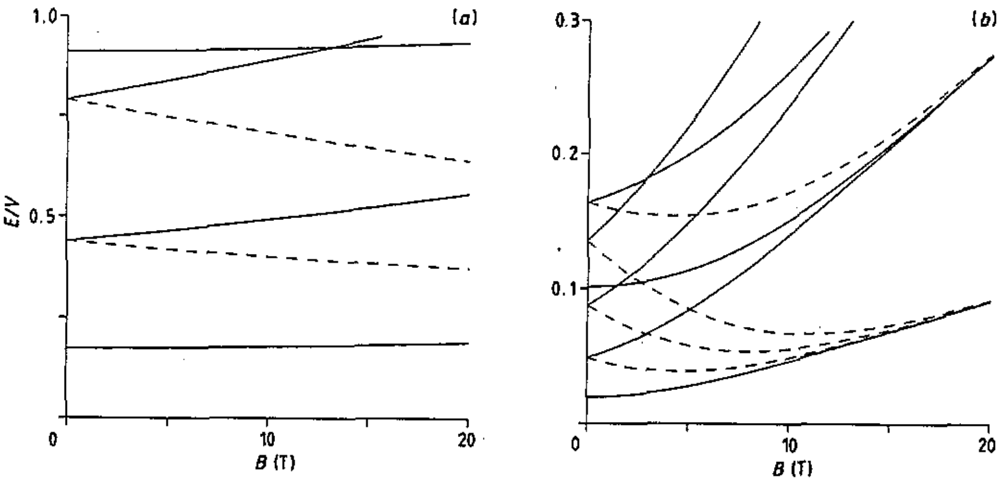

Figure 1. Lowest-order subband energies versus magnetic field for an infinite potential. The subbands are identified by their (m, l) quantum numbers and the sequences start from the lowest-energy subband. (a) corresponds to a wire of radius 100 Å; the (m, l) sequence is $\{(0,0),(1,0),(2,0),(0,1)\}$ for the solid curves and $\{(-1,0),(-2,0)\}$ for the dashed curves. (b) corresponds to R = 300 Å and the sequence is $\{(0,0),(1,0),(2,0),(0,1),(3,0),(1,1)\}$ for the solid curves and $\{(-1,0),(-2,0),(-3,0),(-1,1)\}$ for the dashed curves. The other parameter is $\mu = 6.1 \times 10^{-32}$ kg.

Some of the eigenvalues obtained numerically from (21) are depicted in figure 1 for two different radii. We concentrate our discussion on the curve corresponding to a wire of radius 300 Å. For zero applied magnetic field the states are doubly degenerate except, of course, those correponding to $m = 0$. The application of a magnetic field lifts this degeneracy, with the states characterized by $m > 0$ shifting to higher energies and those characterized by $m < 0$ initially shifting to lower energies. This is just the Zeeman effect. For small magnetic fields the energies are given by

$$E = E_{0m} + \tfrac{1}{2}m\hbar\omega_c \qquad m = 0, \pm1, \pm2, \ldots \tag{26}$$

where E_{0m} is the subband energy at zero magnetic field. In fact, for a given m ($\neq 0$) the difference in energy between the positive and negative states remains $|m|\hbar\omega_c$ at larger fields. For small magnetic fields the $m = 0$ subbands are unaffected since they have zero orbital angular momentum. As the magnetic field increases we see that there is a minimum in the energy for states with $m < 0$ corresponding to fields between 5 and 15 T. The reason for this is as follows. The interaction of an electron with the magnetic field consists of two parts $\hat{H}_1$ and $\hat{H}_2$ given by

$$\hat{H}_1 = (e/\mu)\boldsymbol{A}\cdot\boldsymbol{p} = \tfrac{1}{2}\omega_c\hat{L}_z \tag{27}$$

$$\hat{H}_2 = (e^2/2\mu)A^2 = \tfrac{1}{8}\mu\omega_c^2\rho^2 \tag{28}$$

where $\hat{L}_z$ is the z-component of the orbital angular momentum operator. The interaction $\hat{H}_1$ is responsible for the linear Zeeman splitting. The energy quadratic in B is often ignored in atomic spectroscopy as the expectation value $\langle\rho^2\rangle$ is typically a few square ångströms. Dingle [18] has considered the problem when $\hat{H}_2$ is a small perturbation. In the case of a quantum wire $\langle\rho^2\rangle$ is typically around 150^2 Å^2 and thus $\hat{H}_2$ is not in general negligible. The minima in the energies for states with $m < 0$ occur at a magnetic field such that $\langle\hat{H}_1\rangle = 2\langle\hat{H}_2\rangle$:

$$\pi\langle\rho^2\rangle B = |m|h/e = |m|\Phi_0 \qquad m = -1, -2, -3, \ldots \tag{29}$$

where $\Phi_0 = h/e$ is the fundamental flux quantum. The general nature of the argument leading to (29) suggests that for any form of the confining potential in the wire with cylindrical symmetry, the E–B curve will have a minimum for negative m, and that it will occur at about the field given by (29). We therefore see that the energy minima occur whenever $|m|$ flux quanta are enclosed within the electron's cyclotron orbit. The minima in the subband energies for electrons with negative azimuthal quantum numbers is the main prediction of this paper and ought to occur in other low-dimensional systems in which the carriers have intrinsic orbital angular momentum such as spherical quantum dots.

Comparison of figure 1(a) and 1(b) shows that for $R = 300$ Å the negative-m minima are located at magnetic field values that are quite accessible experimentally, but for $R = 100$ Å they are not. The scaling of the field axis with cylinder radius is clear from (1) and (21): the B scale decreases quadratically with increasing R.

To complete this section we illustrate in figure 2 the radial wavefunctions of the lower-order eigenvalues. It should be noted that the radial wavefunctions for positive and negative values of m are the same. This follows straightforwardly from the fact that their energy difference is always $|m|\hbar\omega_c$. The $m = 0$ wavefunctions are the only ones that are finite on the axis, although they have zero gradient there. The $|m| = 1$ wavefunctions vanish at the origin whilst their gradient is finite; the $|m| = 2$ wavefunctions have zero value and zero gradient at the origin. For higher magnetic fields the radial wavefunctions shift towards the cylinder axis as expected, and this is clearly seen when 2(b) and 2(d) are compared.

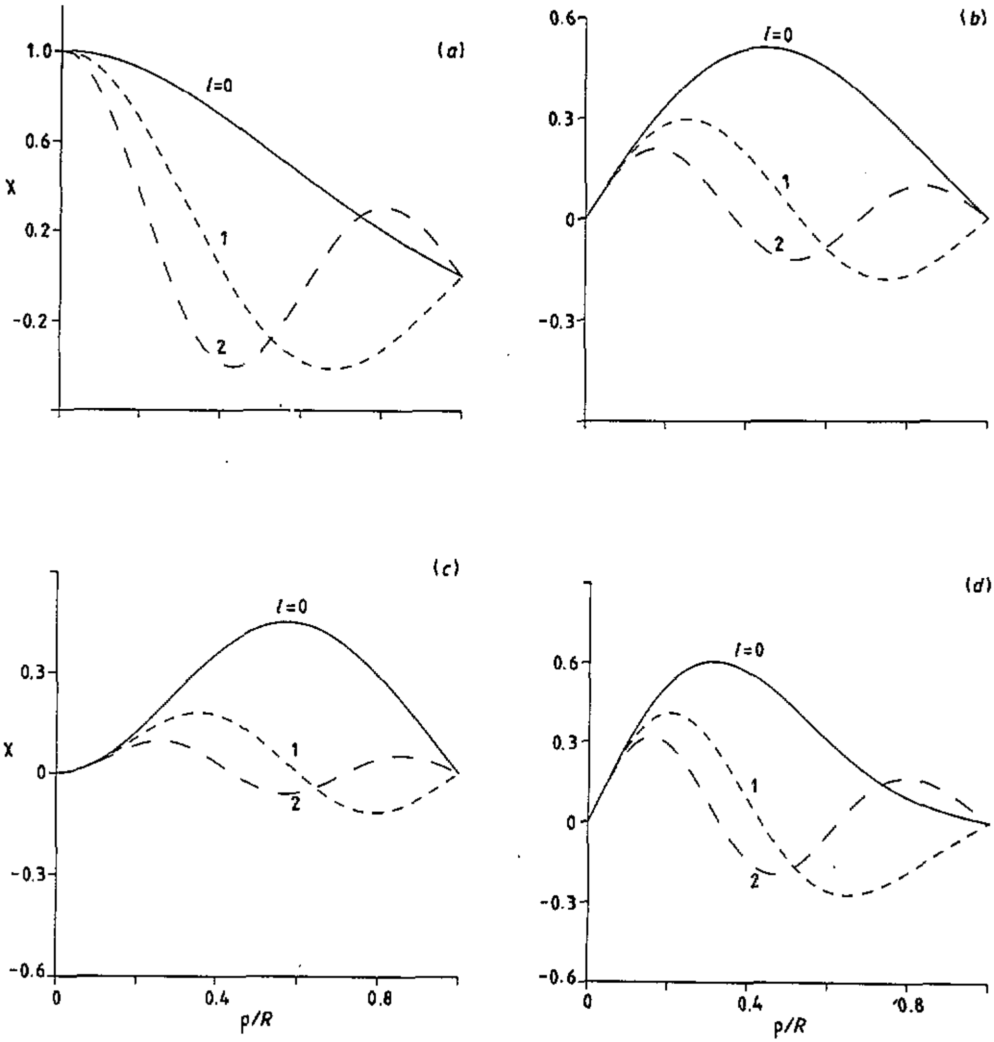

Figure 2. The radial wavefunctions versus ρ/R for an infinite potential well for R = 300 Å. (*a*) $m = 0$, $B = 5$ T, (*b*) $|m| = 1$, $B = 5$ T, (*c*) $|m| = 2$, $B = 5$ T, (*d*) $|m| = 1$, $B = 15$ T.

4. Applied magnetic field, finite step

We now consider the more general situation where the potential takes a finite value V for $\rho > R$; this would be a model for a GaAs quantum wire in Al$-x$Ga$_{1-x}$As, for example. In the outside region, the wave function is (with C a normalization factor)

$$\chi_0 = C \exp(-\xi/2)\xi^{|m|/2} U(\alpha, b, \xi) \tag{30}$$

where ξ is given by (14) and b by (20), U is the solution of the confluent hypergeometric equation that is bounded as $\xi \to \infty$, and α is given by

$$\alpha = (V - E)/\hbar\omega_c + \tfrac{1}{2}(1 + m + |m|). \tag{31}$$

The effective-mass boundary conditions are that χ and $\mu^{-1}\,\mathrm{d}\chi/\mathrm{d}\rho$ are continuous at $\rho = R$; applied to (16) and (30) these lead to the eigenvalue equation

$$\chi_0\chi' - (\mu_1/\mu_2)\chi\chi_0' = 0 \tag{32}$$

where μ_1 and μ_2 are the effective masses of the interior and exterior regions and the prime denotes differentiation with respect to the argument.

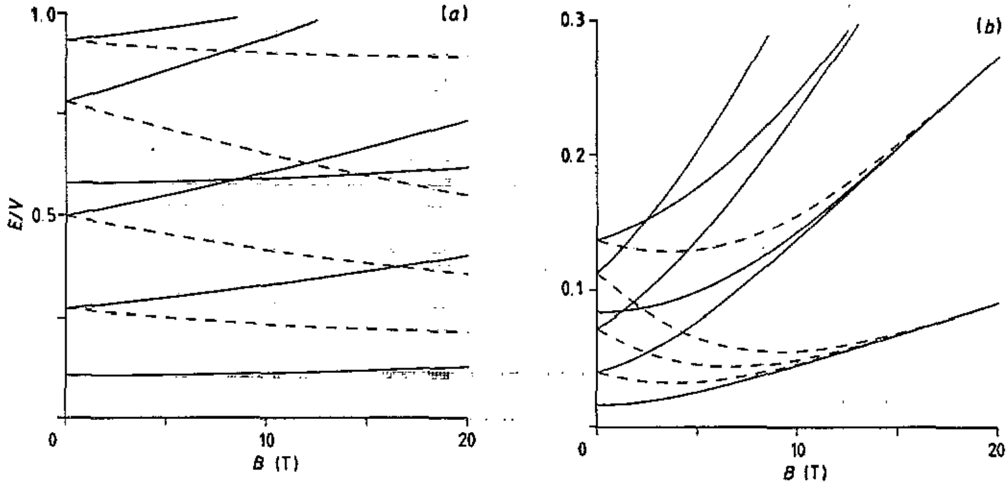

Figure 3. Lowest-order subband energies versus magnetic field for a finite potential well (V = 190 meV) for: (*a*) R = 100 Å with the solid curves corresponding to the sequence $\{(0,0),(1,0),(2,0),(0,1),(3,0),(1,1)\}$ and the dashed curves to $\{(-1,0),(-2,0),(-3,0),(-1,1)\}$; (*b*) R = 300 Å with solid and dashed curve sequences as for figure 1(*b*). The other parameter is μ_2/μ_1 = 1.4.

The general discussion of the eigenvalue equation (32) and in particular the way in which the azimuthal quantum number m enters is the same as in section 3. The zero-field results, which form the $a_c \to \infty$ limit, are given by Constantinou and Ridley. Some curves to illustrate the results are shown in figure 3. Again we concentrate on the low-energy states of the 300 Å wire. The behaviour is similar to that of the infinite wall system. The important point is that the minima in the $m < 0$ curves still exist and occur around the same magnetic fields as before. The main difference between the two cases is that the energies are lower in the case of a finite well as is clear from the uncertainty principle. It is interesting to note that for the 100 Å wire the pairs of confined subbands corresponding to $|m| = 1$, $l = 1$ and $|m| = 3$, $l = 0$, now have energies less than V. The finite-potential wavefunctions are not shown here for brevity. For the low-lying energy levels they are not too different from the infinite-wall wavefunctions although, of course, there is penetration into the barrier.

5. Conclusion

The quasi-one-dimensional subband energies of electrons confined by a cylindrically symmetric square-well potential (both infinite and finite) have been calculated within the effective-mass approximation as a function of applied magnetic field along the axis of the cylinder. A minimum in the energies associated with carriers having negative azimuthal quantum number is predicted. This effect arises whenever the confining potential has cylindrical symmetry and is not restricted to the square-well type. These minima occur whenever $|m|$ quanta of magnetic flux are enclosed within the electron's cyclotron orbit. It should also be noted that a similar effect ought to occur in spherical quantum dots [19] although we do not analyse this system here as we leave this to a future calculation. In fact, this system is closely related to that of a hydrogen-like donor in a magnetic field. Praddaude [20] has investigated the energy levels of hydrogen-like atoms in magnetic fields in which minima in the negative-m states are also predicted.

The closely related work of Makar *et al* [13] is concerned with the eigenfunctions in cylindrical shell, where the electron is confined to the region $R_1 < \rho < R_2$. In that work, the authors develop approximate solutions in terms of Airy functions and give an extended discussion involving limiting and asymptotic forms. In fact an exact solution is possible. We hope to return to a discussion of this at a later date.

Finally, Patel *et al* [21] have applied parallel magnetic fields to a quasi-one-dimensional constriction. Similar experiments in systems where the confining potential has cylindrical symmetry may make it possible to investigate experimentally the behaviour of the subband energy levels as a function of parallel magnetic field.

Acknowledgments

We would like to thank the UK Science and Engineering Research Council for financial support of one of us (NCC) and the University of Botswana for financial support of another (MM). We thank Dr S Monaghan and Dr A J Vickers for useful discussion.

References

[1] Landau L D and Lifshitz E M 1985 *Quantum Mechanics* (Oxford: Pergamon)
[2] Harper P G 1991 *J. Phys.: Condens. Matter* **3** 3047
[3] Klama S 1987 *J. Phys. C: Solid State Phys.* **20** 551
[4] Lee H R, Oh H G, George T F and Um C I 1989 *J. Appl. Phys.* **66** 2442
[5] Bastard G 1984 *Phys. Rev.* B **30** 3547
[6] Mitrovic B, Milanovic V and Ikonic Z 1991 *Semicond. Sci. Technol.* **6** 93
[7] Sakaki H 1980 *Japan. J. Appl. Phys.* **19** L735
[8] Thornton T J, Pepper M, Ahmed H, Andrews D and Davies G J 1986 *Phys. Rev. Lett.* **57** 1769
[9] Berggren K F, Thornton T J, Newson D J and Pepper M 1986 *Phys. Rev. Lett.* **57** 1769
[10] Ismail K, Antoniadis D A and Smith H I 1989 *Appl. Phys. Lett.* **54** 1130
[11] Plaut A S, Lage H, Grambow P, Heitmann D, von Klitzing K and Ploog K 1991 *Phys. Rev. Lett.* **67** 1642
[12] Laux F, Frank D J and Stern F 1988 *Surf. Sci.* **196** 101
[13] Makar M N, Ahmed M A and Awad M S 1991 *Phys. Status Solidi* b **167** 647
[14] Iafrate G J, Kerry D K and Reich R K 1982 *Surf. Sci.* **113** 485
[15] Cibert J, Retroff P M, Donon G J, Pearton S J, Gossard A C and English J H 1986 *Appl. Phys. Lett.* **49** 1275
[16] Constantinou N C and Ridley B K 1989 *J. Phys.: Condens. Matter* **1** 2283
[17] Abramowitz M and Stegun I A (ed) 1965 *Handbook of Mathematical Functions* (New York: Dover)
[18] Dingle R B 1952 *Proc. R. Soc.* A **212** 47
[19] Temkin H, Dolan G J, Parish M B and Chu S N G 1987 *Appl. Phys. Lett.* **50** 413

[20] Praddaude H C 1972 *Phys. Rev.* A **6** 1321
[21] Patel N K, Nicholls J T, Martin-Moreno L, Pepper M, Frost J E F, Ritchie D A and Jones G A C 1991 *Phys. Rev.* B **44** 10973